International Forum on Aeroelasticity and Structural Dynamics
IFASD 2017
25-28 June 2017, Como - Italy

NONLINEAR STATIC AEROELASTIC ANALYSIS OF HIGH-ASPECT RATIO WING BASED ON CFD/CSD COUPLING SOLUTION

Yang Lan[1], Xie Changchuan[1], Yang Chao[1], Zhang Bing[2], Andrea Da Rouch[3]

[1]School of Aeronautics Science and Engineering, Beihang University,
Key Laboratory of Aircraft Advanced Design Technology (Beihang University), Ministry of Industry and Information Technology, Beijing, 100191, China
yanglanby@buaa.edu.cn

[2]School of Mechanical Engineering
Hefei University of Technology, Hefei 230009, China
18056053007@163.com

[3]Faculty of Engineering and the Environment
University of Southampton, Southampton, SO171BJ, United Kingdom
A.Da-Ronch@soton.ac.uk

Keywords: FSI, static aeroelastic, geometrical nonlinear FEM

Abstract: This paper discussed the implementation of a nonlinear static aeroelastic analysis framework based on CFD/CSD coupling method. For fluid-structure interaction (FSI) problems, a conventional serial staggered (CSS) procedure is applied to generate a loosely-coupled scheme. The Reynolds-averaged Navier-Stokes equations are solved for the fluid, and a geometrical nonlinear finite element method is used for the structure. The morphing of the mesh is achieved using a spring-TFI (trans-finite interpolation) hybrid approach with rotation correction. The proposed nonlinear static aeroelastic framework is demonstrated on a very flexible high-aspect ratio wing, which is currently undergoing wind tunnel testing.

1 INTRODUCTION

In recent years, with the development of large flexible aircrafts such as High-Altitude Long-Endurance Unmanned Aerial Vehicles (HALE UAVs), some new problems of aeroelastic analysis of the large aspect ratio wing have arisen. [1] Because of the large flexibility, these aircrafts undergo large deformations under flight loads. On account of the obvious changes of the configuration, the traditional linear analysis based on the small deformation hypothesis is no longer suitable for such cases and it cannot reflect the real physical nature of the large flexible aircrafts [2]. Therefore, nonlinear analysis of both structure and aerodynamics is necessary and a nonlinear aeroelastic framework is required.

For nonlinear aeroelastic problems, CFD/CSD coupling method is fairly effective. Along with the progress of computer performance, aerodynamic calculation by CFD method based on Euler or Navier-Stokes equations and structural analysis based on CSD solution are rapidly improving [3]. The CFD simulation is based on geometrically exact aerodynamic model and precise governing equations of fluid, considering various nonlinear factors such as transonic flow, large angle of attack and viscosity. In the meantime, structure geometric nonlinear problems cause by large structural displacement can be solved by FEM. Therefore, aeroelastic analysis based on CFD/CSD coupling method is developed.

For the coupling strategy, both partitioned and monolithic procedures have been investigated by researchers. In a monolithic scheme, the fluid and structure are treated as a single system. [4]P. Le Tallec and J. Mouro solved the FSI problems with large structural displacements considering the fluid and the structure as a unique continues medium and using an associated arbitrary Lagrangian Eulerian (ALE) formulation. In a partitioned procedure for FSI, the fluid and structure subsystem can be dealt with independently and thus the existing fluid/structure solvers can be used directly, resulting in a more widely application. Based on a loosely-coupled scheme, [5] Hitoshi Arizono and Carlos E.S. Cesnik conducted a research on computational static aeroelasticity using nonlinear structures and aerodynamics models and also attained satisfying results. [6] Yang Guowei etc. studied computational methods and engineering applications of static/dynamic aeroelasticity using CFD/CSD coupling solution.

The moving grid technology is a significant part of the CFD/CSD coupling solution for aeroelastic problems. Especially for large structural deformation problems, an effective and efficient mesh morphing technology is necessary. Mesh deformation algorithms such as transfinite interpolation (TFI), spring analogy and radius basis function (RBF) are applied to aeroelastic analysis where the interface of fluid and structure is changing according to the elastic deformation. [7] Zhang Bing etc. proposed a hybrid dynamic mesh method combining TFI, spring method as well as rotation correction, and obtained deformed mesh of satisfying orthogonality and smoothness, which is suitable for large deformation situations and used in this paper.

The present paper is aimed at building up a nonlinear static aeroelastic framework of high-aspect ratio wing under large deformation and providing an accurate method for static aeroelastic problems in engineering. Considering the large structural deformation of high-aspect ratio wing, CFD method based on Reynolds-averaged Navier-Stokes equations is exploited to obtain aerodynamic loads of high fidelity and geometric nonlinear finite element method is used to conduct the structure analysis. Based on the loosely coupling solution, the fluid equations and the structural equations are solved successively and separately. A spring-TFI hybrid dynamic mesh method with rotation correction is used to generate the new mesh of the deformed wing. The numerical results of a high-aspect ratio wing indicate that the proposed framework of static aeroelasticity is validated and can be applied to more complex engineering fields.

2 COUPLING STRATEGY FOR PARTITIONED PROCEDURE

For FSI problems, partitioned procedures are of great advantages for various reasons [8]. It reduces the computational complexity per time-step and meanwhile achieves software modularity. In this paper, we adopt a loosely-coupled solution algorithm to analyze nonlinear static aeroelastic problems. The fluid equations and the structure equations are solved successively and separately.

Firstly, aerodynamic loads are calculated by CFD method. The solution can be accomplished by commercial fluid solvers, such as ANSYS Fluent, and therefore easily implemented in industry analysis. The original multi-block structured grids can be generated with ICEM or GridGen software. In this paper, the solution is based on Reynolds-averaged Navier-Stokes equations and the Spalart-Allmaras one-equation turbulence model is employed. [9] The fluid equations are

$$\frac{\partial U}{\partial t}+\frac{\partial F}{\partial x}+\frac{\partial G}{\partial y}+\frac{\partial H}{\partial z}=J \tag{1}$$

where U is the solution vector. F,G,H are flux vectors and J represents the source term.

For the structural analysis, static deformation is calculated using geometrically nonlinear FEM. Geometric nonlinearities are based on the kinematic description of the body and the strain should be defined in terms of local displacement. Geometric nonlinear effects are prominent in two different aspects: (1) geometric stiffening due to initial displacements and stresses, and (2) follower forces due to load changes with structure displacements. In this paper, the updated Lagrange formulation (ULF) is used for structural geometrically nonlinear analysis and [10] the primary equation is

$$\left({}^{t}\mathbf{K}_{L}+{}^{t}\mathbf{K}_{NL}\right)\mathbf{u}={}^{t+\Delta t}\overline{\mathbf{Q}}-{}^{t}\mathbf{F}_{A} \tag{2}$$

where ${}^{t+\Delta t}\overline{\mathbf{Q}}$ is the incremental outer force, including the aerodynamic force, engine thrust, and gravity at the new time step. The term ${}^{t}\mathbf{F}_{A}$ is the equivalent inner force in the structure. The stiffness matrix in Eq. (2) can be decomposed into a linear part ${}^{t}\mathbf{K}_{L}$ and a nonlinear part ${}^{t}\mathbf{K}_{NL}$. The linear part is only related to the structure itself, whereas the nonlinear part is related to the deflected configuration, load condition and strain quality, each of which should be updated in each computational step.

In each step of iteration, information of force and displacement needs to be transferred between aerodynamic and structural models. To be specific, aerodynamic loads obtained from CFD

analysis should be interpolated to the structure, satisfying virtual work principle. After the structure calculation, the aerodynamic configuration has to be updated according to the displacement of structure grids and thus the new CFD mesh needs to be regenerated correspondingly. The data communication will be discussed specifically in section 3. The above-mentioned process is repeated until the deformation of the wing converges. Figure 1 illustrates the process of the loosely-coupled procedure.

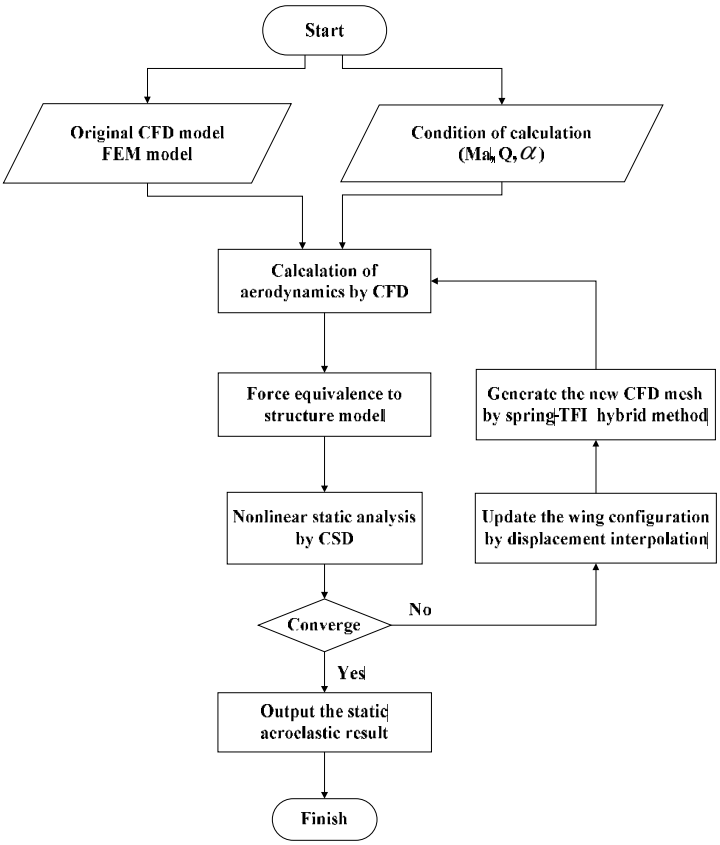

Figure 1 Nonlinear static aeroelastic analysis flow chart

3 INTERPOLATION AND MESH MORPHING ALGORITHM

3.1 SURFACE SPLINE INTERPOLATION

In this paper, surface spline interpolation [11] is applied to transfer displacement and load information between structure and aerodynamic models.

Considering n structural grid points described by $\mathbf{X}_S$ and the corresponding displacements $\mathbf{U}_S$, the interpolation relationship can be described as

$$\mathbf{A}_S\mathbf{C} = \mathbf{W}_S \tag{3}$$

where $\mathbf{A}_S$ is a constant matrix calculated by the given information of the structure grids and $\mathbf{W}_S = \begin{bmatrix} \mathbf{0}_{3\times4} & \mathbf{U}_S^T \end{bmatrix}^T$ contains the information of the displacements of the given grids. $\mathbf{C}$ is the coefficient matrix of the surface spline fitting function. Thus, the displacements of the m grid points of the aerodynamic model can be obtained by

$$\mathbf{U}_A = \mathbf{A}_A \mathbf{A}_S^{-1} \mathbf{W}_S \tag{4}$$

where $\mathbf{A}_A$ is a constant matrix according to the coordinates of the given aerodynamic grids.

Ultimately, the interpolation relationship between structure and aerodynamic models yields

$$\mathbf{U}_A = \mathbf{G}\mathbf{U}_S \tag{5}$$

where the spline matrix for displacement interpolation $\mathbf{G}$ is obtained by removing the first four columns of $\mathbf{A}_A \mathbf{A}_S^{-1}$.

When it comes to force equivalence, the virtual work principle has to be satisfied:

$$\delta \mathbf{U}_A^{\mathrm{T}} \mathbf{F}_A = \delta \mathbf{U}_S^{\mathrm{T}} \mathbf{F}_S \tag{6}$$

where $\delta\mathbf{U}_A, \delta\mathbf{U}_S$ are arbitrary virtual displacement of aerodynamic grids and structure grids, respectively. The terms $\mathbf{F}_A, \mathbf{F}_S$ are the load vectors on aerodynamic and structure models. Substitute Eq. (5) into Eq.(6), and we obtain the interpolation relationship of forces:

$$\mathbf{F}_S = \mathbf{G}^{\mathrm{T}} \mathbf{F}_A \tag{7}$$

3.2 MESH MORPHING ALGORITHM

In the case of large deformations, the traditional TFI dynamic mesh method may cause problems of orthogonal properties. In this paper, spring-TFI hybrid dynamic mesh method with rotation correction is used to generate the new mesh on the basis of the new wall grids updated by surface spline interpolation, preparing for CFD calculation of the deformed wing.

For multiblock structured mesh, the dynamic mesh calculation can be divided into two parts: the relative motion of blocks and the displacements of internal nodes. For motions among blocks, a set of springs are used to connect the corner nodes of different blocks. The displacements of the corner nodes are obtained by solving equilibrium equations.
For displacements of internal nodes, considering cases of large deformation, each block is split into some sub-blocks and springs are positioned on the corners of sub-blocks to improve the orthogonality and smoothness of the mesh, illustrated in Figure 2.

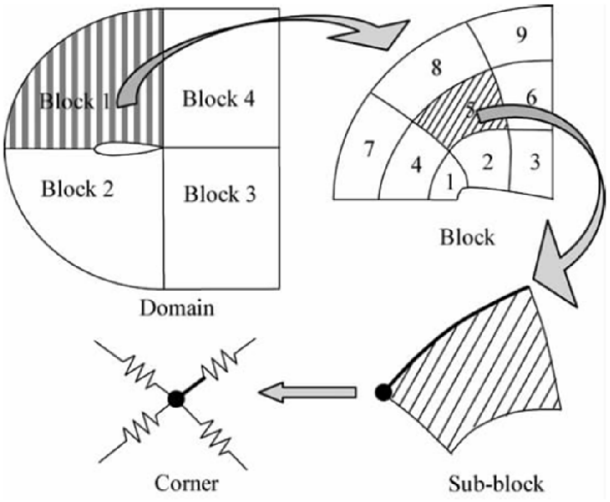

Figure 2 Sketch map of mesh block splitting method

The equilibrium equation of each corner node is:

$$-\sum_{j=1}^{NE_i} k_{i,j}\Delta\mathbf{x}_i + \sum_{j=1}^{NE_i}(k_{i,j}\Delta\mathbf{x}_j) = 0 \tag{8}$$

where $\Delta\mathbf{x}_i$ is the displacement vector of node i and $\Delta\mathbf{x}_j$ is the displacement vector of the j th node which is connected with node i; NE_i is the quantity of springs connecting node i; $k_{i,j}$ is the stiffness of the spring element connecting node i and node j, which is usually set as the reciprocal of the distance between the two nodes. The more sub-blocks are divided, the smoother the deformed mesh will be but at larger computational expenses. Given that the displacements of the sub-block inner nodes are calculated by TFI method, the block is usually divided into 2 to 8 pieces in each direction.

The primary equation of TFI interpolation method in 3D case is

$$\Delta\mathbf{x}_{i,j,k} = \mathbf{U} + \mathbf{V} + \mathbf{W} - \mathbf{UV} - \mathbf{VW} - \mathbf{UW} + \mathbf{UVW} \tag{9}$$

$$\mathbf{U} = (1-\alpha_{i,j,k})\Delta\mathbf{x}_{1,j,k} + \alpha_{i,j,k}\Delta\mathbf{x}_{\mathrm{imax},j,k} \tag{10}$$

$$\mathbf{V} = (1-\beta_{i,j,k})\Delta\mathbf{x}_{1,j,k} + \beta_{i,j,k}\Delta\mathbf{x}_{\mathrm{i},j\,\mathrm{max},k} \tag{11}$$

$$\mathbf{W} = (1-\gamma_{i,j,k})\Delta\mathbf{x}_{1,j,k} + \gamma_{i,j,k}\Delta\mathbf{x}_{\mathrm{i},j,k\,\mathrm{max}} \tag{12}$$

where α,β,γ are normalized arc coordinates in three directions of the structured mesh.

To consider the rotation of the mesh, some correction is made to improve the orthogonality. The rotation vector of nodes can be calculated on the basis of displacements of boundary nodes:

$$\mathbf{R}_i = \frac{1}{NE_i}\sum_{j=1}^{NE_i}\mathbf{R}_{i,j} \tag{13}$$

$$\mathbf{R}_{i,j} = \arccos\left[\frac{\left(\mathbf{x}_j - \mathbf{x}_i\right)\cdot\left(\mathbf{x}_{j_2} - \mathbf{x}_{i_2}\right)}{\left\|\mathbf{x}_j - \mathbf{x}_i\right\|_2\left\|\mathbf{x}_{j_2} - \mathbf{x}_{i_2}\right\|_2}\right]\cdot\frac{\left(\mathbf{x}_j - \mathbf{x}_i\right)\times\left(\mathbf{x}_{j_2} - \mathbf{x}_{i_2}\right)}{\left\|\mathbf{x}_j - \mathbf{x}_i\right\|_2\left\|\mathbf{x}_{j_2} - \mathbf{x}_{i_2}\right\|_2} \tag{14}$$

When rotation vectors of boundary nodes are obtained, the rotation vectors of the internal nodes can be interpolated by TFI method. Additionally, considering that there may be multiple rotation topological structure, the rotational displacements of internal nodes should be superposed.

4 NUMERICAL RESULTS

In order to illustrate the theoretical modeling process and verify the applicability of the framework proposed in this paper, here a static aeroelastic analysis of a very flexible high-aspect ratio wing is presented as a numerical example.

Figure 3 shows the structure model of our study. It is a trapezoidal wing with a low sweep angle of 3.4° and a high aspect ratio of 18.65. The semi span of the wing is 1542.1mm and the length of root chord is 263mm. A supercritical airfoil with camber and thickness is used in this study. In addition, there is a preliminary twist angle of 2° along the span, which means the actual angle of attack of the tip is smaller than the root. To analyze aeroelastic problems, a finite element model is built in MSC. Nastran, shown in Figure 3 (b). The frequency of the 1st mode (1st vertical bending mode) is 3.36Hz.

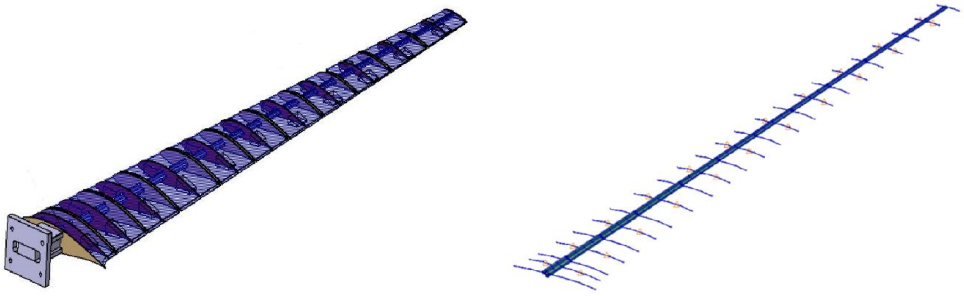

(a) CATIA model (b) Structural finite element model

Figure 3 Calculation model

Figure 4 presents the CFD mesh of the original aerodynamic model, generated by Ansys ICEM. The number of grid points is approximately two million.

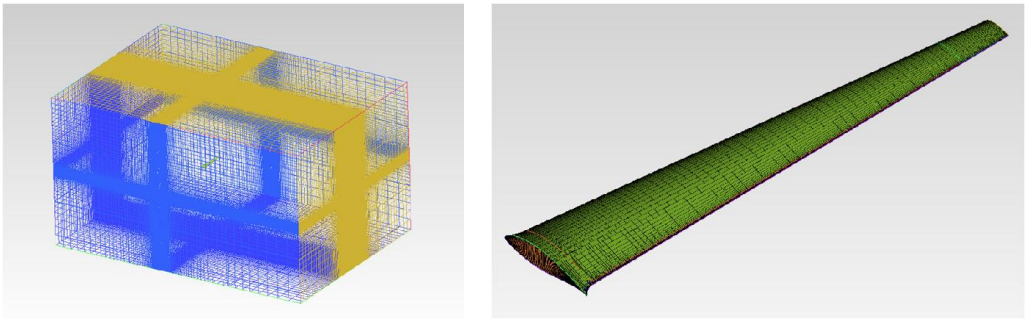

(a) global view (b) wing surface mesh

Figure 4 CFD mesh of the flow field

Setting the freestream velocity as 30m/s and the angle of attack of the wing root as 5 degree, the numerical results of the nonlinear static aeroelastic analysis are provided as following.

First, aerodynamic analysis of the original wing is conducted. The total lift of the wing is 110.57N while the total drag is 5.95N, which makes the lift/drag ratio 18.56. Figure 5 illustrate distribution of lift and drag along the span, respectively. Here the wing is analyzed separately, with no symmetry condition. Thus the lift increases at first and then decreases along the span, reaching the maximum at 26% of the span from the root. In order to provide specific load information of the wing, Figure 6 gives the pressure contour of the wing surface.

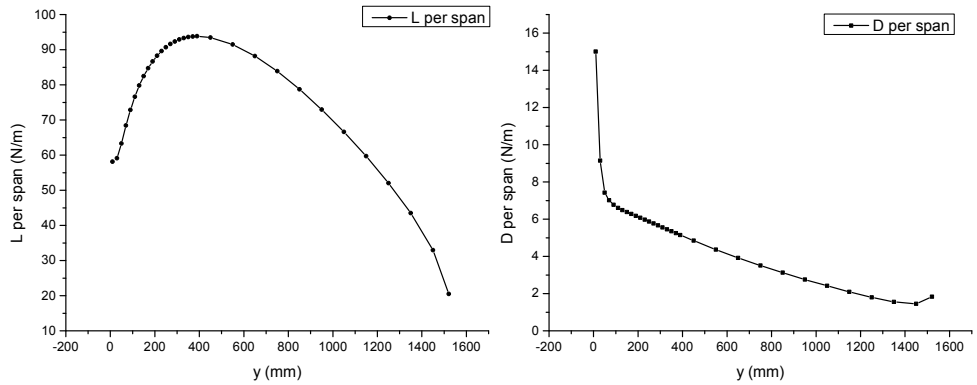

(a) Lift distribution (b) Drag distribution

Figure 5 Load distribution along the span

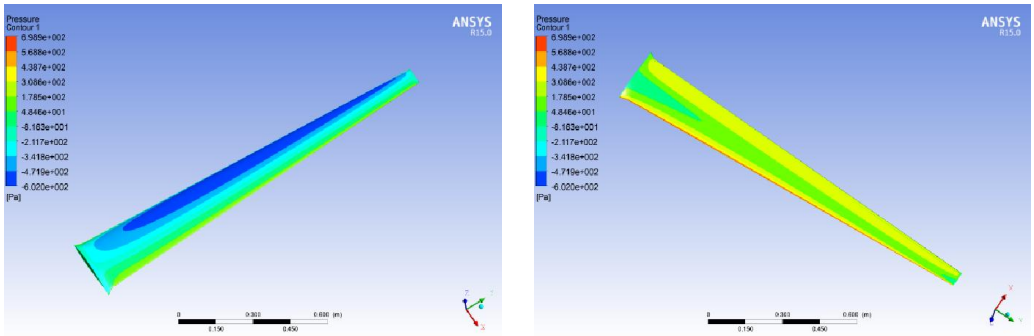

(a) Upper wing surface (b) Lower wing surface

Figure 6 Pressure contour of the undeformed wing

According to the process of nonlinear static aeroelastic analysis showed in Figure 1, the aerodynamic loads as well as the structural displacements shall be updated successively during

the aeroelastic iteration. The wing surface produces deformation along with the structural deflection and torsion, and the surface mesh of the wing is generated by surface spline interpolation, shown in Figure 7. Then the CFD mesh is updated to calculate the new flow field, as Figure 8 shows. The results indicate that aerodynamic configuration of the wing changes significantly under flight loads, which highlights the importance of accurate aerodynamic analysis.

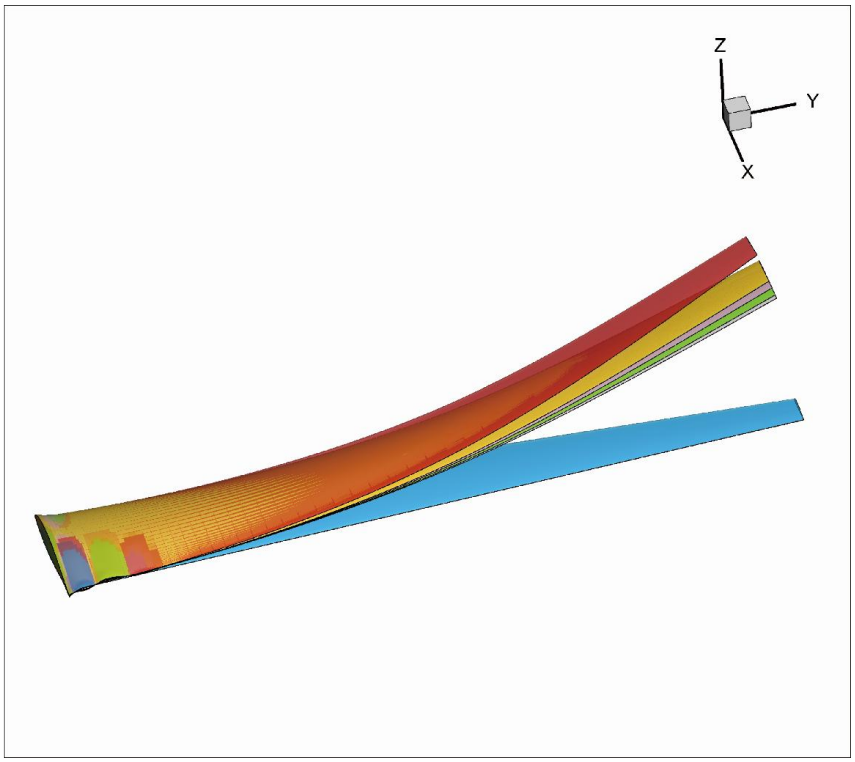

Figure 7 Deformed wing surfaces during iteration

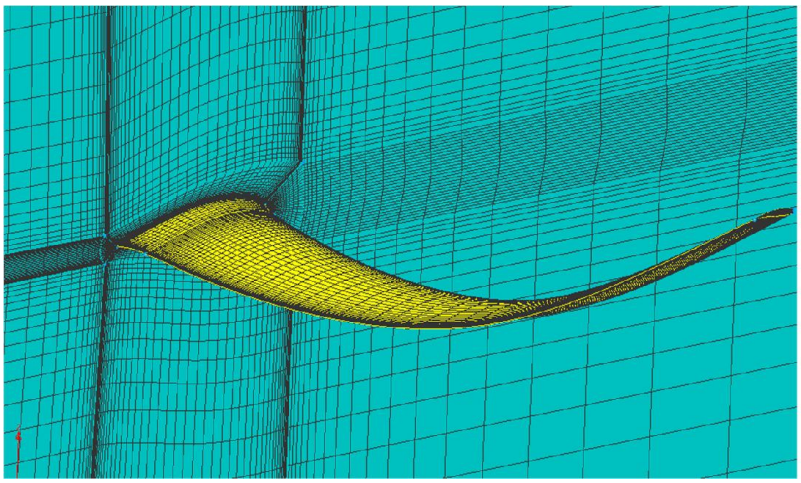

Figure 8 Updated CFD mesh of the deformed wing

Figure 9 shows the pressure coefficient distribution of the chord section y=0.7m and y=0.4m, from which we can see the differences among the iterations. Figure 10 presents the pressure contour of the aeroelastic equilibrium configuration. The total lift is 102.56N while the total drag is 5.74N, which makes the lift/drag ratio 17.87. Large structural deformation diminishes the affective area of the wing and changes the aerodynamic configuration, which affects loads on the structure in return. Additionally, due to the large deflection of the wing, lateral forces in

negative direction of y axis arise and result in deformation in y direction, which differs from the linear aeroelastic analysis.

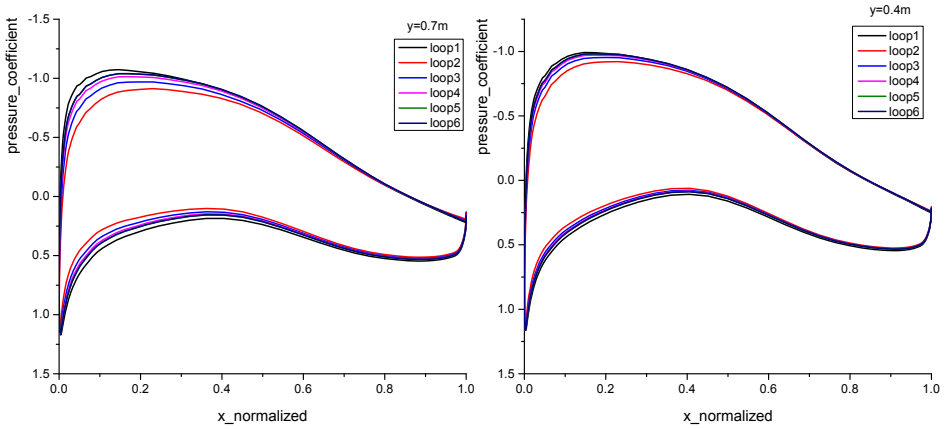

Figure 9 Pressure coefficient of two chord sections

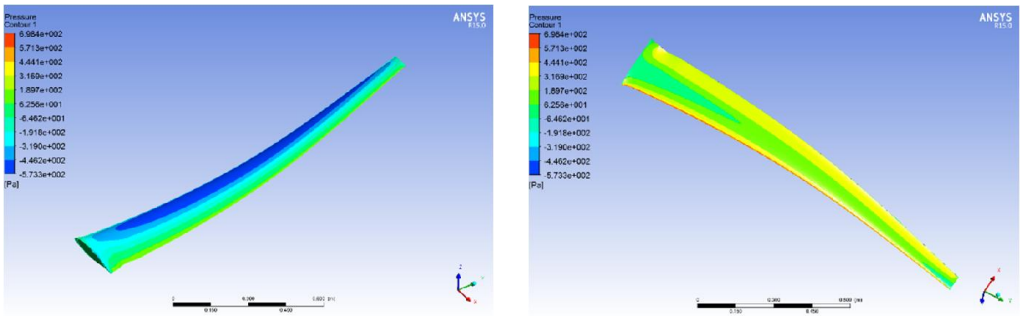

(a) Upper wing surface (b) Lower wing surface

Figure 10 Pressure contour of the equilibrium configuration

Figure 11 and Figure 12 shows the variation of the vertical and horizontal displacements and the elastic twist of the main beam structural grid points during iteration. After six calculation loops, the results of displacements and torsion angles gradually converges. When it comes to the convergence, the maximum vertical displacement reaches 348mm, making 20% of the semi span while the maximum lateral displacement produces 3.5% of the semi span. Geometrical nonlinear FEM is used to calculate the structure deformation. Tangent stiffness matrix as well as following loading makes the structure analysis for large deformation more accurate and reasonable.

For wings with a swept angle, deflection often causes negative torsion, which means the affective angle of attack decreases and part of the aerodynamic loads is discharged. In this case, the affective angle of attack of the wing tip is 1.3° smaller than that of the root, illustrated in Figure 12.

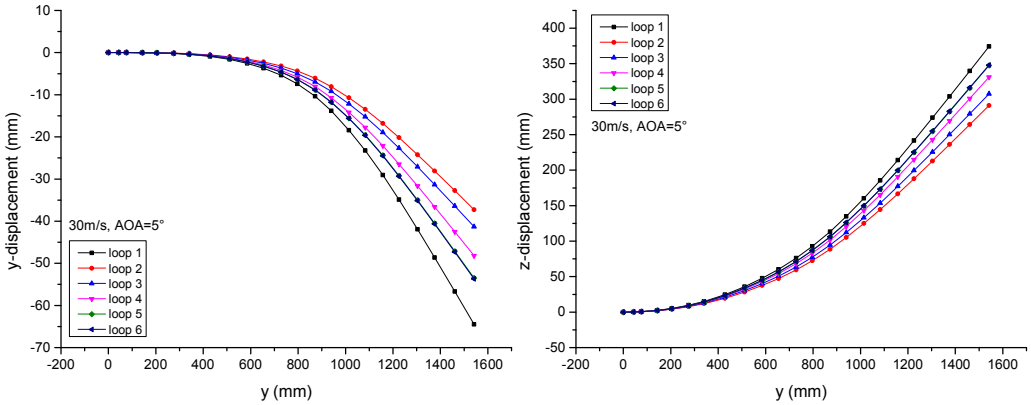

Figure 11 Displacements of main beam structural grid points during iteration

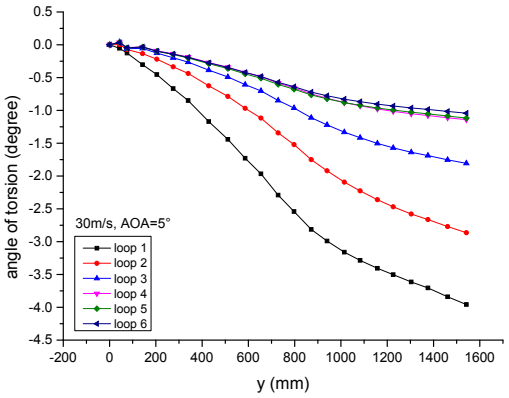

Figure 12 Torsion angles of main beam structural grid points during iteration

5 CONCLUSION

In this paper, a framework of nonlinear static aeroelastic analysis is established and applied on a flexible high-aspect ratio wing. The CFD method based on RANS equations is exploited to obtain aerodynamic load of high fidelity and geometric nonlinear finite element method is used to conduct the structural analysis. In order to generate the new CFD mesh of the wing after large deformation, a spring-TFI hybrid dynamic mesh method with rotation correction is applied, on the basis of the new wing surface mesh obtained by surface spline interpolation. Following the staggered procedures of FSI solution, the fluid equations and the structure equations are solved successively and separately. During the iteration loops, the displacements as well as the loads gradually converge and the equilibrium configuration presents large vertical deformation. Considering the changes of aerodynamic configuration and the effects of geometrical nonlinearities synthetically, the results of static aeroelastic analysis produces accuracy and the framework can also be applied to engineering fields readily.

6 REFERENCE

[1] Xie Changchuan, Liu Yi**,** Yang Chao. “Theoretic Analysis and Experiment on Aeroelasticity of Very Flexible Wing”, Science China Technological Sciences, 2012, 55(9): 2489-2500.

[2] Xie Changchuan, Wang Libo, Yang Chao, Liu Yi. “Static Aeroelastic Analysis of Very Flexible Wings Based on the Non-Planar Vortex Lattice Method”, Chinese Journal of Aeronautics. 2013,26(3):514-521

[3] O O Bendiksen, “Modern developments in computational aeroelasticity”, Proceedings of the Institution of Mechenical Engineers, 218(2004)157-177

[4] P. Le Tallec and J. Mouro. “Fluid structure interaction with large structural displacements”, Computer methods in applied mechenics and engineering, 190(2001)3039-3067

[5] Hitoshi Arizono and Carlos E.S. Cesnik. “Computational Static Aeroelasticity Using Nonlinear Structures and Aerodynamics Models”. 54th AIAA/ASME/ASCE/AHS/ASC Structures, Structural Dynamics, and Materials Conference. AIAA 2013-1862, April 8-11, 2013, Boston, Massachusetts.

[6] Yang Guowei, Zheng Guannan and Li Guibo. “Computational methods and engineering applications of static/dynamic aeroelasticity based on CFD/CSD coupling solution”, Science China, Vol.55, No.9:2453-2461, 2012, doi:10.1007/s11431-012-4935-1

[7] Zhang Bing, Han Jinglong. “Spring-TFI hybrid Dynamic mesh method with rotation correction”, Acta Aeronautica et Astronautica Sinica, 2011,32(10):1815:1823

[8] Charbel Farhat, Kristoffer G. van der Zee, Philippe Geuzaine. “Provably second-order time-accurate loosely-coupled solution algorithms for transient nonlinear computational aeroelasticity”, Computer Methods in Applied Mechenics and Engineering, 195(2006)1973-2001, doi:10.1016/j.cma.2004.11.031

[9] John D. Anderson, “Computational Fluid Dynamics – the basics with applications”, MCcGraw-Hill, Inc; 1995.

[10] Wang XC, Shao M. “Foundation and numerical method of finite element method”, Beijing: Tsinghua University Press; 1997[Chinese]

[11] Xie Changchuan, Yang Chao, Surface Splines Generalization and Large Deflection Interpolation, Journal of Aircraft, Vol. 44, No. 3, May-June, 2007, 1024-1026

ACKNOWLEDGEMENT

This work was supported by the National Key Research and Development Program (2016YFB0200703).

COPYRIGHT STATEMENT